Preparation and Evaluation of Recombinant Human Erythropoietin Loaded Tween 80-Albumin Nanoparticle for Traumatic Brain Injury Treatment

Yuanfeng Xue[1],*
Junhong Ding[1],*
Yulong Liu[2]
Yuchun Pan [ORCID][1]
Penglai Zhao[3]
Zhiwen Ren[1]
Jian Xu[1]
Liangliang Ye[1]
Ying Xu[2]

[1]Department of Neurosurgery, Nanjing Lishui People's Hospital, Zhongda Hospital Lishui Branch Southeast University, Nanjing 211200, People's Republic of China; [2]College of Pharmacy, Jiangsu University, Zhenjiang 212013, People's Republic of China; [3]Department of Neurosurgery, Brain Hospital Affiliated to Nanjing Medical University, Nanjing 210029, People's Republic of China

*These authors contributed equally to this work

Objective: Traumatic brain injury (TBI) is a serious health problem with few available treatment options. Rh-erythropoietin (rh-EPO) is a potential therapeutic drug for TBI, but it cannot cross the blood–brain barrier (BBB) directly. In this regard, a novel strategy to deliver rh-EPO for enhanced TBI treatment is via the development of Tween 80 modified albumin nanoparticles using electrostatic spray technology.

Methods: The rh-EPO loaded Tween 80 modified albumin nanoparticles (rh-EPO-Tw-ABNPs) were prepared by electrostatic spray technology, while the process parameters were optimized via a single factor design. Investigation of physicochemical properties, bioactivity and stability of rh-EPO-Tw-ABNPs was carried out. The in vitro release and biocompatibility with nerve cells were also analyzed. The in vivo brain targeting efficiency, brain edema relieving effect and the expression of aquaporin 4 (AQP4) and glial fibrillary acidic protein (GFAP) in the brain were evaluated in TBI model rats.

Results: The particle size of optimal rh-EPO-Tw-ABNPs was about 438 ± 45 nm, with a zeta potential of -25.42 ± 0.8 mv. The average drug loading ratio of rh-EPO-Tw-ABNPs was 21.3 ± 3.7 IU/mg with a relative bioactivity of $91.6 \pm 4.1\%$. The in vitro release of rh-EPO from the nanoparticles was rather slow, while neither the blank Tw-ABNPs nor rh-EPO-Tw-ABNPs exhibited toxicity on the microglia cells. Furthermore, in vivo experiments indicated that the rh-EPO-Tw-ABNPs could enhance the distribution of EPO in the brain and relieve brain edema more effectively. Moreover, compared with an rh-EPO injection, the rh-EPO-Tw-ABNPs could increase the AQP4 level but reduced GFAP expression in the brain with more efficiency.

Conclusion: The rh-EPO-Tw-ABNPs could enhance the transport of rh-EPO into the brain with superior therapeutic effect for TBI.

Keywords: traumatic brain injury, rh-erythropoietin, Tween 80 modified albumin nanoparticle, electrostatic spray technology

Introduction

Traumatic brain injury (TBI) is usually induced by external forces with an annual impact on approximately 2.5 million Americans.[1] TBI can cause serious damage to brain tissue, for example parenchymal injury, cerebral hemorrhage and axonal shear, which in turn culminate in a high mortality and disability rate, with the survivors often suffering from physical, cognitive and psychosocial dysfunction.[2–4] Unfortunately, an

Correspondence: Yuanfeng Xue; Ying Xu
Tel +8613951706820; +8651185038451
Email 672455219@qq.com;
ingyx@sina.com.cn

effective treatment for TBI is still lacking. Various animal TBI models have been designed, viz., the control cortical impact (CCI) model, fluid percussion injury (FPI), penetrating ballistic-like brain injury (PBBI), and weight drop models (the Feeney weight-drop and Marmarou weight-drop models).[3,5] The Feeney weight-drop model is a classical method to establish a rat TBI model. According to the animal spinal cord injury model, Feeney designed a free-falling brain injury device, and successfully established a focal brain injury model by using a heavy object falling directly from a certain height to impact the animal head.[6] It was widely used in the establishment of TBI animal models because of its simplicity, good control and quantification as well as the closeness of injury mechanism to human TBI.[7,8]

Erythropoietin (EPO) is an endogenous hormone produced by stress under hypoxic conditions and a major regulatory factor that controls red blood cell production,[9–11] wherein it may increase oxygen delivery and reduce brain damage.[12,13] Preclinical experiments have confirmed that recombinant human erythropoietin (rh-EPO) can protect nerves, resist apoptosis, promote vascular regeneration, and reduce cerebral edema,[14] which have been widely studied in cases of stroke, cerebral ischemia, and TBI. However, rh-EPO is a large glycosylated protein which cannot cross the blood–brain barrier (BBB) directly as the transport of drugs across BBB requires specific vector transport or internalization that has a saturation point.[15] In addition, the required concentration of rh-EPO to effectively protect the brain from injury is high, but the amount of rh-EPO that reaches the brain through systemic administration is limited, making it difficult to meet the treatment requirement. Some researchers have found that nanotechnology could enhance transport of drugs and increase the distribution of drugs in an injured brain area by passing usual BBB routes.[16,17] Chen et al. showed that an rh-EPO nano preparation was 10 times more effective as a neuroprotector in rat hypoxic and cerebral ischemic models than an ordinary rh-EPO dosage form.[18] Per our extensive search, few studies have used rh-EPO nano preparation to treat TBI.

Albumin has attracted widespread attention as a drug delivery system owing to its advantages of no immune response, good biocompatibility and biodegradability. Albumin-paclitaxel nanoparticle (Abraxane®) was approved by the US FDA in 2005. Nanoparticles have also been used as the vehicle to deliver drugs into the brain.[19] Besides, Tween 80 is an amphiphilic non-ionic surfactant which has been proven to promote drugs to cross the BBB via low density lipoprotein (LDL)-mediated endocytosis.[20–23]

Conventional albumin micro/nanoparticle preparation technologies, such as emulsification, high-pressure homogenization and nab-techniques, usually have thermogenesis or require chemical cross-linkage, which negatively affect the stability of protein drugs. Electrostatic spray is a method of atomizing liquid or polymer solution through electrostatic force.[24,25] It has been widely used in materials science, tissue engineering and other fields, wherein there are preliminary developments in the pharmaceutical field that can achieve direct and continuous preparation of drug-loaded microspheres[26,27] (Figure 1). Compared with other methods, the advent of electrostatic spray technology has been advantageous especially due to its simple one step formation and avoidance of heat and organic solution, making it ideal for protein drugs.[28]

Herein, we sought to develop rh-EPO loaded Tween 80 modified albumin nanoparticles (rh-EPO-Tw-ABNPs) as a new strategy to improve its TBI therapeutic effect. We first applied the electrostatic spray technology in fabricating the albumin nanoparticles and optimized the formulation process. The characteristics of the rh-EPO-Tw-ABNPs were investigated, while the biocompatibility of the carrier and biological activity of the protein drug were detected. The in vivo brain targeting efficiency and brain edema relieving effect were evaluated in the rat using the Feeney weight-drop model.

Materials and Methods

Bovine serum albumin was purchased from Nanjing Assistant Research Biotechnology Co., Ltd (Nanjing, China). Tween 80 was bought from Sinopharm Chemical Reagent Co., Ltd (Shanghai, China). The Rh-EPO was obtained from Harbin Pharmaceutical Group Bioengineering Co., Ltd (Harbin, China). ELISA kits were supplied by Yubo Biological Technology Co., Ltd (Shanghai, China). Microglia cells (BFN60805942) and astroglia (BFN213825) were procured from Qingqi Biological Technology Co., Ltd (Shanghai, China). Motor neurocytes (HopCell-MN-24) were provided by Hopstem Biotechnology LLC (Zhejiang, China).

Method
Preparation of rh-EPO-Tw-ABNPs

Bovine serum albumin (200 mg) and polyethylene oxide (PEO, average MV 300000, 20 mg) were dissolved in 9 mL of double distilled water (DD water) under magnetic stirring. Then, rh-EPO (6000 IU) and 1 mL of Tween 80 were added to obtain a transparent solution with
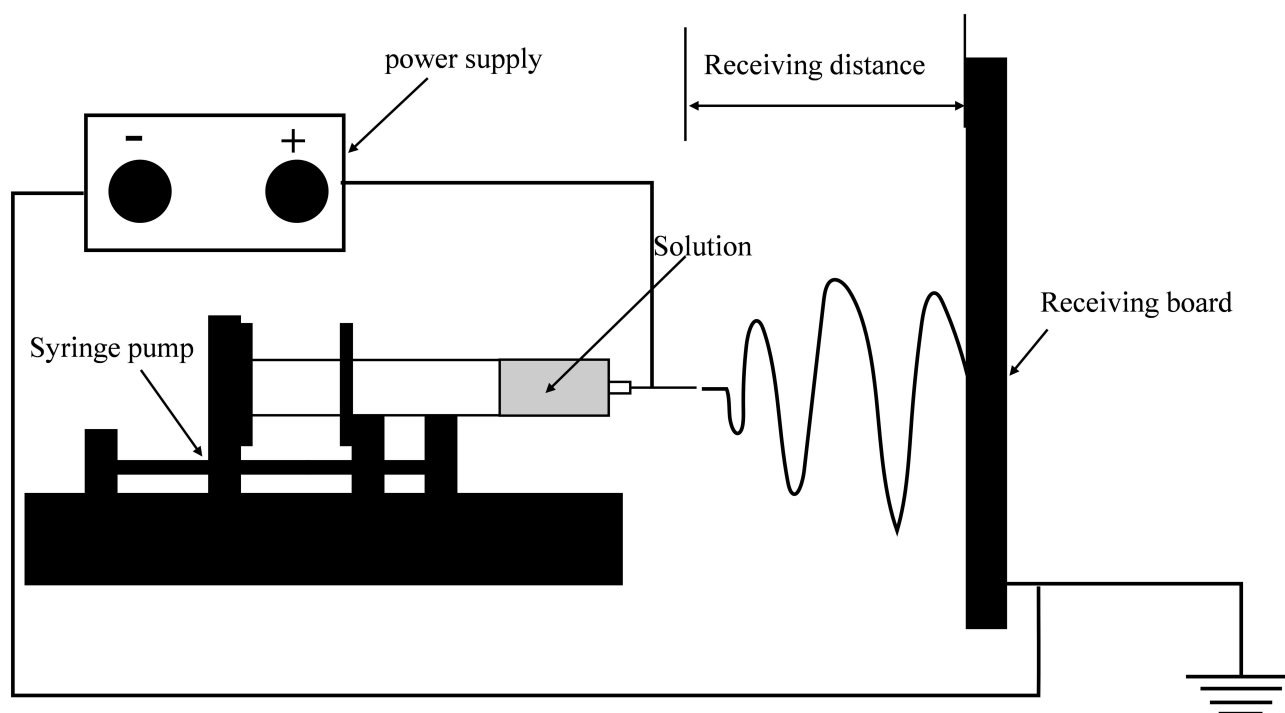
Figure 1 The Schematic diagram of the electrostatic spray technology.

temperature controlled below 4 °C. The mixed solution was added into a 10 mL syringe and sprayed by a 30G gun onto the foil receiving board. The temperature of the machine was set at 0 °C, while the humidity was set to 20%. The powder on the foil was collected to obtain rh-EPO-Tw-ABNPs.

Optimization of Processing Parameters
Effect of Voltage
The rh-EPO-Tw-ABNPs were fabricated under different voltages (20, 24 and 28 kv), while the optimized voltage was selected according to the particle size which was determined via dynamic light-scattering method (DLS, 90puls PALS, Brookhaven, USA).

Effect of Flow Rate
Flow rate is an important parameter that affects the morphology. The different flow rates (0.5 mL/h and 1 mL/h) were investigated to prepare the nanoparticles. Also, the morphology was observed and used as the evaluation index. Rh-EPO-Tw-ABNPs were installed on the sample table with conductive tape. Before measurement, the surface of the tape was coated with gold before observing the samples via scanning electron microscopy (SEM) (S-4800 Ⅱ FESEM, Hitachi High-Technologies, Japan).

Effect of Receiving Distance
The receiving distance is an important parameter that affects the morphology and directly influences the uniformity of nanoparticles. We examined the impact of different receiving distances (15, 20 and 25 cm) with SEM to determine the optimal receiving distance.

Characterization of rh-EPO-Tw-ABNPs
Particle Size, Zeta Potential and Morphology
Dynamic light-scattering (DLS) method was used to determine the particle size and zeta potential of rh-EPO-Tw-ABNPs. Briefly, rh-EPO-Tw-ABNPs (2 mg) were put into 20 mL DD water to obtain the suspension. The particle size and zeta potential were determined by 90Plus PALS particle size analyzer (Brookhaven, USA). A drop of rh-EPO-Tw-ABNPs sample (500 μg/mL) was put on a copper grid and then stained with 2% phosphotungstic acid. The morphology was observed with transmission electron microscopy (TEM) (Tecnai 12, Philips, Holland).

Bioactivity, Drug Loading Efficiency and Stability Study
An appropriate amount of rh-EPO-Tw-ABNPs (5 mg) was dissolved in DD water (100 mL) prior to the detection of the bioactivity and content of rh-EPO via an ELISA kit. The drug loading ratio was calculated by the following

equation: Drug loading ratio= W_{rh-EPO}/W_S, where W_{rh-EPO} was the IU of rh-EPO detected in nanoparticles, W_S was the weight of nanoparticles. The rh-EPO-Tw-ABNPs were stored at −4 °C and an appropriate amount of samples were withdrawn at different time points (0, 24, 48, 72 and 96 h) to determine the particle size and bioactivity.

In vitro Release

Specific amounts of rh-EPO-Tw-ABNPs and rh-EPO injection (containing 500 IU of rh-EPO) were accordingly transferred into the dialysis bag (MW 200 KD, MD55-200000-01), and were put into 500 mL of pH 7.4 PBS, under stirring at 37 °C. Aliquots (1 mL) of samples were withdrawn at the scheduled time and the same volume of the release medium was supplemented at the same time. The concentration of rh-EPO in the released medium was determined using an ELISA kit and the cumulative release curves were drawn.

Safety Evaluation
Cell Cultures

All the cells were cultured in Dulbecco's Modified Eagle's Medium-HG (DMEM-HG; Gibco, Carlsbad, CA, USA) supplemented with fetal bovine serum (FBS, 10% v/v; Gibco), penicillin (100 U/mL) and streptomycin (100 μg/mL). Next, the cells were cultured in an incubator (Thermo Electron Corporation) operating at 37 °C under 5% CO_2. The use of the cells was approved by the Jiangsu University Ethics Committee.

The safety of the fabricated nanoparticles was evaluated on three kinds of cells. Briefly, the microglia cells, motor neurocyte and astroglia were seeded in 6-well plates at a density of 1×10^4 cells/well for 24 h, respectively. After that, the culture medium was removed and replaced with the medium containing rh-EPO-Tw-ABNPs or blank-Tw-ABNPs, respectively. After 48 h of incubation, the cells' morphologies were observed under inverted optical microscope (ECLIPSE Ti-E, Nikon Corporation, Japan).

Brain Targeting Efficiency
Construction of Animal Models

All the experimental protocols were approved by Jiangsu University Ethics Committee for Animal Experimentation following the principles of laboratory and animal care of the University (UJS-IACUC-AP-2020040222).

Male Sprague-Dawley (SD) rats (6~8 weeks old, 220~250 g) were obtained from Jiangsu University Animal Center (Zhenjiang, China) and were fasted for 12

h with unrestricted access to water ad libitum prior to the experiment.

Feeney weight-drop model was established on male Sprague-Dawley rats as reported in the literature.[7,8] Briefly, the rats were anesthetized with pentobarbital sodium (50 mg/kg). Then, the animals were placed in the prone position while the head and limbs were fixed on the operating table, before the scalp was shaved. After routine iodophor disinfection, the scalp was cut along the median line before the periosteum was peeled off, and the left parietal bone exposed. A round bone window with a diameter of about 5 mm was drilled out at 1.5 mm behind the left coronal suture and 2.5 mm beside the median line to keep the dura mater intact. A circular steel plate pad (4.5 mm in diameter and 3.5 mm in thickness) was placed outside the dura mater. A 20 g steel weight was impacted on the steel plate pad along the sleeve from a height of 30 cm, causing local cerebral contusion and laceration in the parietal lobe. Next, the bone window was closed with bone wax, while the scalp was sutured. The injured rats were fed in the original cage after waking up. The rats in the sham-operated control group received the same operation, but no injury was caused by hitting the bar.

Brain Targeting Efficiency of rh-EPO-Tw-ABNPs

The accumulation levels of rh-EPO in the brain were detected with Western blotting to evaluate the targeting efficiency of the Tween 80 modified albumin nanoparticles. Briefly, TBI model rats were operated on as above and divided into 4 groups (n=5, each group): sham-operated, TBI+ saline, TBI+ rh-EPO solution and TBI+ rh-EPO-Tw-ABNPs groups. The rats in the saline, rh-EPO solution or rh-EPO-Tw-ABNPs groups were i.p. administered (5000 IU/kg) 30 min after TBI impact. Twenty-four hours later, the rats were sacrificed after anesthesia and the brain was harvested. Then, the supernatant was aspirated after the brain issue was homogenized and centrifuged (2000 g, 10 min). Next, the proteins were extracted using RIPA buffer. Afterwards, the BCA kit was applied to detect the total protein concentration. An aliquot of each sample was mixed with 10% sodium dodecyl sulfate-polyacrylamide gel electrophoresis (SDS-PAGE) loading buffer and transferred to polyvinylidene difluoride (PVDF) membrane via wet rotation method. Next, the PVDF membranes were blocked with 5% skimmed milk at room temperature for 1 h. Subsequently, the membrane was incubated overnight with rabbit anti-human antibodies comprising of B-actin (1:1000), EPO at 4 °C. The goat

anti-rabbit IgG (1:1000, Sigma) marked by HRP was added to the PVDF membranes and incubated for 1 h at room temperature, followed by washing three times with PBS. Then, quantitative analysis was conducted via Image J image processing software.

Brain Edema Relieving Study

The brain edema relieving effects of rh-EPO formulations were detected in the TBI model. The TBI model and dose regimen were the same as stated above. The rats were sacrificed after 24 h of rh-EPO administration, while the brain was rapidly removed and divided along the midline. Then, the wet weight of ipsilateral hemisphere was taken immediately, following drying at 65 °C for 72 h to obtain dry weight. The brain water content was calculated using the following equation: brain water content (%) = (wet weight-dry weight)/wet weight × 100%.

The time and dose effect of the rh-EPO nanoparticles on edema relieving were further evaluated. Briefly, the TBI model rats were randomly divided into three groups (n=15, each group) which were administered with saline, or rh-EPO nanoparticles (2500 and 5000 IU/kg), respectively. Five rats in each group were sacrificed at different time points (12, 24 and 36 h) after TBI, and their brain water contents were detected as stated above.

Expressions of Aquaporin 4 (AQP4) and Glial Fibrillary Acidic Protein in Brain (GFAP)

The expressions of AQP4 and GFAP in brain were evaluated by Western blot analysis and immunohistochemical (IHM) study. The TBI model and dose regimen were the same as described above. Twenty–four hours after the administration, the mice were sacrificed after anesthesia and the brain was harvested. The Western blot analysis was performed as stated above, except that the membrane was incubated with rabbit anti-human antibodies comprising AQP4 and GFAP at 4 °C. The quantitative analysis was conducted by Image J image processing software.

An IMH study was conducted to observe the expression levels of AQP4 and GFAP in the brain . Streptomyces avidin peroxidase linkage method was used to test the chemical staining of brain tissue. The brain tissue was cut into sections (4 μm), dewaxed with xylene and hydrated with gradient ethanol. The sections were immersed in 0.1 M citrate buffer solution for 12 min before addition to 3% H_2O_2 solution to remove endogenous peroxygenase for 10 min. After the non-

specific antigen was blocked by normal goat serum, AQP4 or GFAP polyclonal antibody (1:200) was added, and incubated overnight at 4 °C. The slices were rinsed with PBS solution three times. Next, the film was dripped with polymer and incubated at 37 °C for 20 min. After washing by PBS three times, goat anti rabbit IgG labeled with horseradish peroxidase (1:500) was added and incubated at 37 °C for 25 min, followed by PBS washing sequence. Afterwards, DAB solution was added to develop color for 10 min, and was re-dyed with hematoxylin, dehydrated and sealed, before it was finally observed under a Nikon Eclipse E600 microscope (Nikon Co., Tokyo, Japan).

Hematoxylin and Eosin (H&E) Evaluation

The TBI model and dose regimen were the same as stated above. The mice were sacrificed 24 h after administration and the brains were harvested. The brains were fixed in 4% POM solution at 4 °C for 24 h, prior to washing with PBS. Next, the fixed brains were embedded in paraffin. The average section thickness of 5 μm was histologically evaluated with H&E staining. Then, the images of histopathological examination were observed under a Nikon fluorescence microscope (Nikon, Tokyo, Japan).

Statistical Analysis

Statistical differences between means were determined by SPSS using the Student's t-test, where p<0.05 was considered statistically significant. Values are reported as mean ± SD.

Results and Discussion
Preparation of rh-EPO-Tw-ABNPs and Parameter Optimizations

Electrostatic spray technology is usually used to fabricate polymer materials. This technology has not been used to prepare albumin nanoparticles because albumin lacks elasticity and ductility. Accordingly, PEO was added to increase spheroidization. The voltage, flow rate and receiving distance were important parameters in electrostatic spray, which had relatively high influence on the morphology, particle size and uniformity of the fabricated nanoparticles.[29]

Voltage

As shown in Table 1, the particle size of the nanoparticles decreased as the voltage increased, while particles prepared with 28 kv had a relatively smaller size. It is likely that the higher voltage may result in small droplets, thereby leading to a smaller particle size.[30] It was speculated that the voltage

Table 1 Particle Size and Zeta Potential of rh-EPO-Tw-ABNPs Prepared at Different Voltages (Mean ± SD, n=3)

Voltages	Lognormal Median Diam. By Number (nm)	Polydispersity	Zeta Potential (mv)
20kV	637 ± 48	0.302 ± 0.021	−28.81 ± 3.11
24kV	562 ± 31	0.270 ± 0.042	−21.45 ± 2.52
28kV	458 ± 29	0.245 ± 0.039	−24.92 ± 3.84

directly affects the traction force of the spindle droplet in the electrostatic spray. The higher the traction force, the smaller the size of the droplet.[31] At high voltage, the droplet mode is better than the spray mode, as it could accelerate the droplet formation speed and make the droplet size smaller.[32] However, when the voltage was too high, the sprayed droplet was difficult to solidify and then sprayed as a liquid. Due to this, 28 kv voltage was selected.

Flow Rate

The influence of the flow rate on the morphology of the particles is shown in Figure 2. The particles sprayed at 0.5 mL/h displayed a round shape without obvious adhesion (Figure 2A). However, the particles sprayed at 1 mL/h showed a significant agglomeration phenomenon (Figure 2B). Flow rate is another important parameter that affects the morphology of microspheres. When the flow rate was faster than the volatilization rate, the solvent might not volatilize from the droplet in time, wherein it may lead to agglomeration.[33]

Meanwhile, when the flow rate was too low, the preparation process may take too much time, which might affect product efficiency.[34] Therefore, the flow rate of 0.5 mL/h was selected.

Receiving Distance

In the electrostatic spray process, the receiving distance directly affects the electric field intensity, and then influences the atomization degree and the flying time of the droplet.[35] On the other hand, the larger receiving distance can provide enough time for the jet to be fully stretched, which is also conducive to the evaporation of solvent, so as to reduce the particle size. Meanwhile, an increase in the receiving distance usually reduces the electric field strength, which weakens the droplet atomization, thus increasing the particle size.[36] As shown in Figure 3, the diameter of the microspheres with a 20 cm (Figure 3A) receiving distance was more uniform than those of 25 cm (Figure 3B). The shorter receiving distance of 15 cm was also investigated, however, the solvent could not volatilize in time while the sprayed droplet could not solidify under 15 cm of receiving distance. Possibly, the smaller receiving distance may affect the flight time of the jet under the strong electric field, resulting in insufficient time for the formation of the droplet, or the solvent of the droplet cannot be completely volatilized, culminating in serious agglomeration of the particles. Therefore, the receiving distance was determined as 20 cm.

In summary, the optimized electrostatic spraying parameters were as follows: voltage of 28 kv, flow rate of 0.5 mL/h, and receiving distance of 20 cm.
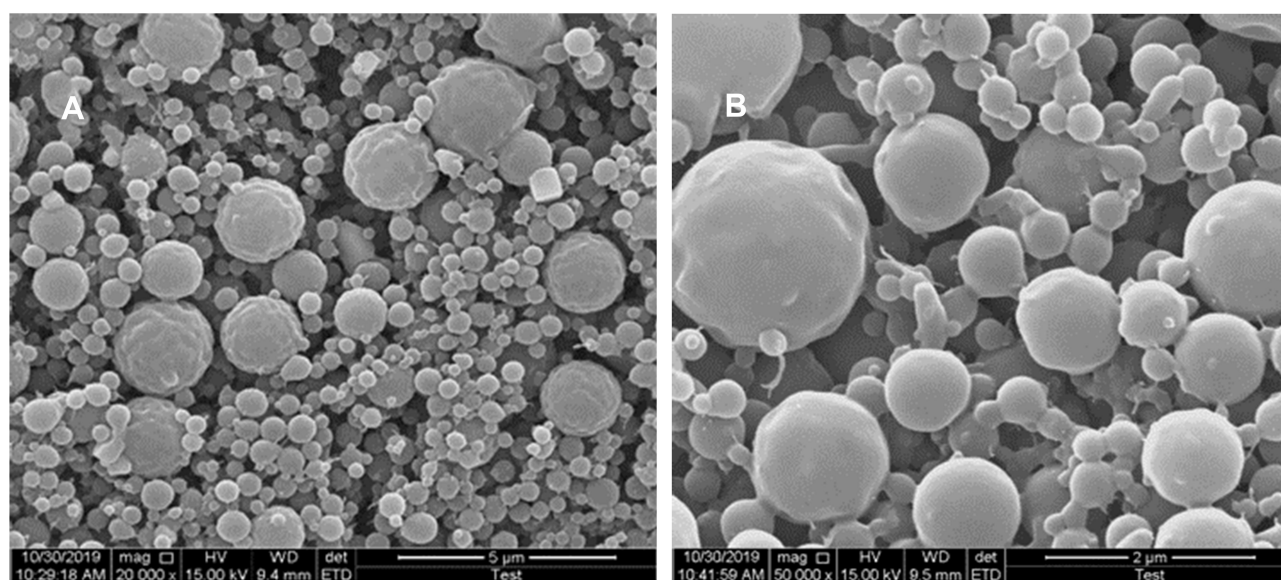

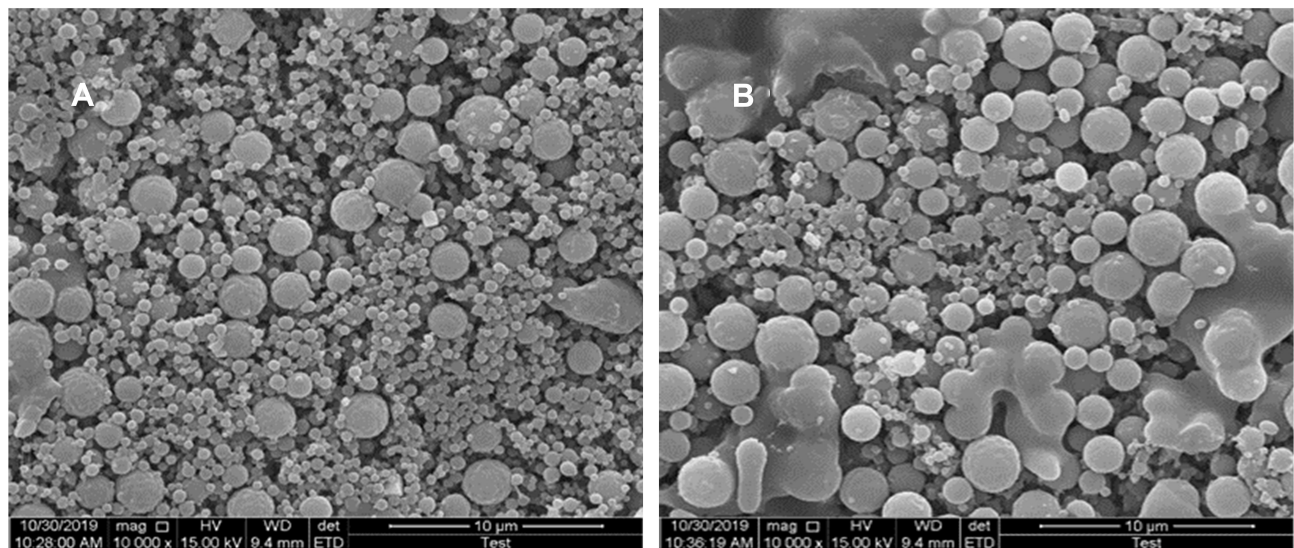**Figure 2** SEM photograph of rh-EPO-Tw-ABNPs prepared by different flow rates (**A**) 0.5 mL/h; (**B**) 1 mL/h.

8500

International Journal of Nanomedicine 2020:15

Figure 3 SEM photograph of rh-EPO-Tw-ABNPs prepared by different acceptance distances (**A**) 20 cm; (**B**) 25 cm.

Characterization of rh-EPO-Tw-ABNPs

The TEM showed that rh-EPO-Tw-ABNPs prepared via optimized formulation had a round shape with a particle size of 450 nm, as shown in Figure 4A. This was close to the result of DLS with a particle size of 438±45 nm and the zeta potential of −25.42±0.8 mv. The isoelectric point of the albumin was about 4.5, therein, the albumin nanoparticle was negatively charged under physiological conditions.[37] As displayed in a SEM photograph, most of the particles were spherical without obvious adhesion, however, formation of some large particles might have been due to voltage fluctuation in the initial stage (Figure 4B). The average drug loading ratio of rh-EPO-Tw-ABNPs was 21.3± 3.7 IU/mg with the relative bioactivity being 91.6 ± 4.1%, which indicated that the preparation process was mild and had very little influence on the bioactivity of the protein drug. The rh-EPO-Tw-ABNPs exhibited potential stability in 96 h. Thus, no significant change in the particle size and protein bioactivity was observed during the investigation period (Figure 4C).

In vitro Release Study

It can be observed from Figure 4D that the release of rh-EPO injection was very quick, thus reaching 80% at 20 min, while that of rh-EPO-Tw-ABNPs was nearly 65%. Moreover, the
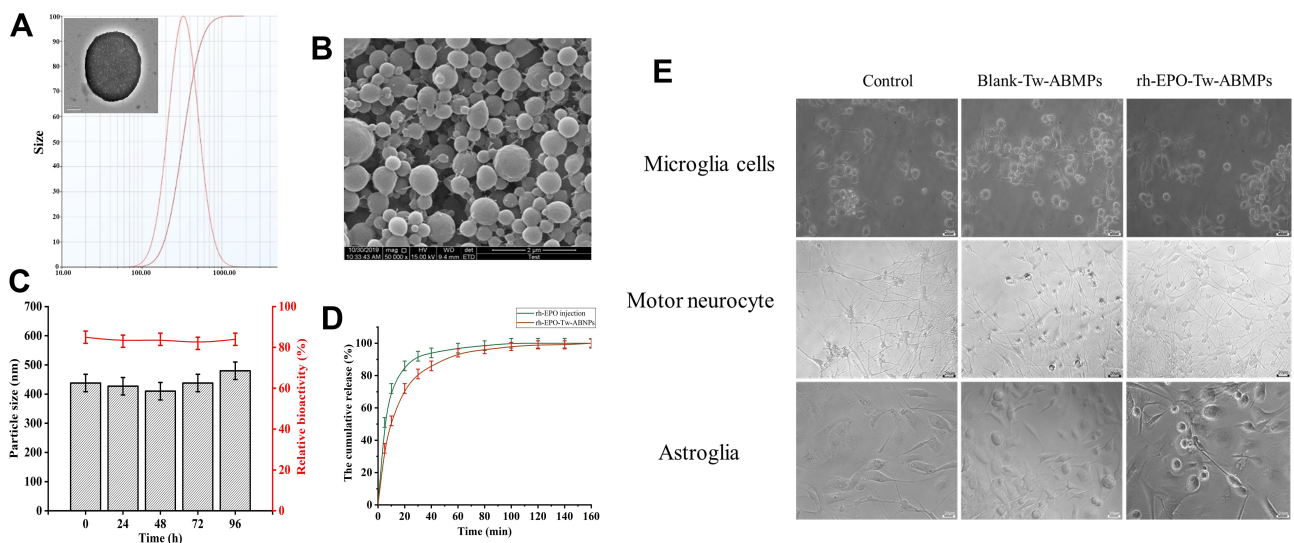

Figure 4 (**A**) TEM and DLS photographs of rh-EPO-Tw-ABNPs. (**B**) SEM photograph of rh-EPO-Tw-ABNPs. (**C**) The stability of rh-EPO-Tw-ABNPs. (**D**) In vitro release of rh-EPO injection and rh-EPO-Tw-ABNPs in PBS medium. (**E**) Photographs of the microglia cells, motor neurocyte and astroglia treated with culture medium (control), blank-Tw-ABNPs and rh-EPO-Tw-ABNPs, respectively.

cumulative release of rh-EPO injection reached approximately 100% at about 50 min. While the release of rh-EPO from the nanoparticles was rather slow, a complete release was attained at about 120 min. The results indicated that the albumin nanoparticles exhibited a slow-release effect. The surface modification of albumin on nanoparticles can also enhance the sustained release of the drug.

Safety Evaluation on Nerve Cells

As displayed in Figure 4E, compared with the control group, the brain and neuron cells, including the microglia cells, motor neurocyte and astroglia, that were treated with the fabricated nanoparticles with or without drug exhibited good morphology, which means the brain and nerve cells could maintain good condition after treatment with blank vehicle or rh-EPO-Tw-ABNPs. In recent years, the biocompatibility of nanoparticles with microglia has been widely studied, amidst serving as a sensitive marker to evaluate the toxicity of exogenous toxicants.[38,39] The results indicated that rh-EPO-Tw-ABNPs had no toxicity on the brain and nerve cells.

Brain Targeting Efficiency of rh-EPO-Tw-ABNPs

Western blot analysis was used to determine the EPO level in the brain after different treatments. The EPO band could be observed clearly in sham-operated and TBI+ saline groups and the EPO level of TBI groups was lower than the sham-operated group (Figure 5A and B), which indicated that EPO was endogenously distributed in the brain, while the EPO level in the brain would be lowered when TBI occurred. Meanwhile, the EPO levels in TBI model rats treated with rh-EPO solution or rh-EPO-Tw-ABNPs increased significantly. Notably, the TBI model rats in the rh-EPO-Tw-ABNPs group exhibited higher EPO level in comparison with the rh-EPO solution. Previous research suggested that coating Tween 80 on nanoparticles resulted in increased amounts of drugs crossing the BBB.[40] The results indicated that rh-EPO-Tw-ABNPs could enhance the transport of rh-EPO across the BBB and improve the brain targeting efficiency of the protein drug.

Brain Edema Relieving

As indicated in Figure 5C, the TBI model was successfully constructed with the brain water content of rats increasing substantially. The TBI-saline group displayed the highest brain water content with the sham-operated groups exhibiting the lowest. The changes of brain water content represented the condition of brain edema. According to the literature, edema

may cause cerebellar hernia, decrease cerebellar blood flow, and accelerate apoptosis of neurons, as well as further aggravate the nerve injury after TBI, but rh-EPO effectively relieved brain edema.[41] Consistent with existing literature, both rh-EPO solution and rh-EPO-Tw-ABNPs groups showed the effect on reducing the brain water content of TBI rats, while rh-EPO-Tw-ABNPs possessed the most efficient effect. Collectively, these observations indicated that rh-EPO-Tw-ABNPs could relieve brain edema more effectively which may be mainly attributed to the enhanced transport of rh-EPO by the nanoparticles to the brain. The dose and time effect of the rh-EPO-Tw-ABNPs on brain edema relieving were further evaluated. As presented in Figure 5D, the high dose group (5000 IU/kg) showed significantly decreased brain water content compared with the low dose group at 12, 24 and 36 h post-TBI. This indicated that the edema relieving effect could enhance the concentration of the rh-EPO nanoparticles raised. According to existing literature, 5000 IU/kg had already been proven as an effective dose in the models of central nervous system (CNS) injuries,[42,43] in addition, the safety concerns of the rh-EPO may be elevated if the dose were too high. In this case, the higher dose was not considered in our study. The water content of the TBI model rats was over 80% at 36 h after trauma. As the literature reports, diffuse brain edema can be detected as early as the first hour post-injury, and may constantly increase at least for 3 days in TBI rats.[41,44] Rh-EPO-Tw-ABNPs treatment decreased the brain water content of the TBI rats for almost 36 h, which indicated that the nanoparticles had a sustained effect on relieving the edema.

The Expressions of AQP4 and GFAP in the Brain

AQP4 is a water-channel protein expressed in the brain, predominantly in astrocyte foot processes surrounding capillaries, which plays a significant role in maintaining brain water homeostasis.[45,46] In comparison with the sham-operated group, it could be seen from the Western blot and IMH results that AQP4 level of peri-lesional areas was decreased when TBI occurred (Figure 5A, B and E). Moreover, the AQP4 level in the brain of TBI model rats treated with rh-EPO solution or rh-EPO-Tw-ABNPs rose again, especially in the rh-EPO-Tw-ABNPs group. There are different opinions about the change in the AQP4 level of TBI model animals. Sun et al. observed that AQP4 expression was upregulated after traumatic brain injury,[47] however, Ke et al. reported that AQP4 expression was downregulated.[48] According to some reports, the AQP4-deficient mice are less prone to develop cytotoxic edema, but
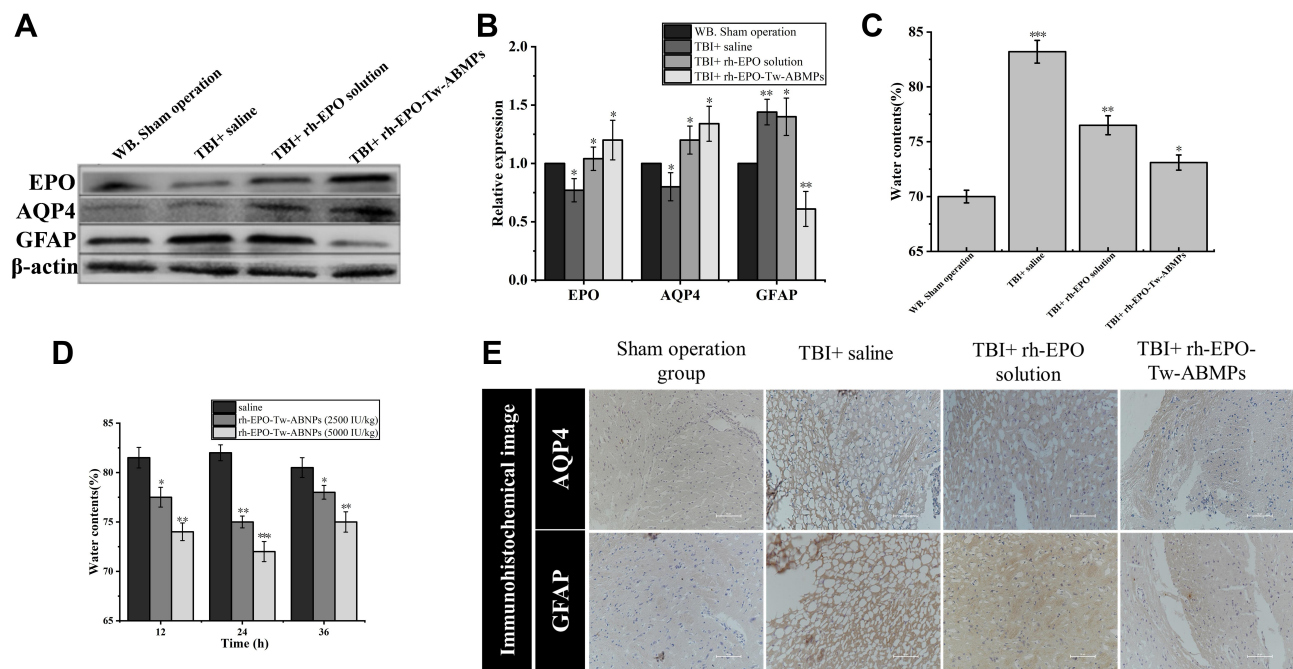
Figure 5 (**A**) Western blotting of EPO, AQP4, GFAP, and β-actin treated with sham operation, TBI+ saline, TBI+ rh-EPO solution, TBI+ rh-EPO-Tw-ABNPs. (**B**) Quality analysis of Western blotting by Image J. (*P<0.05, **P<0.01, compared with sham group). (**C**) The brain water content of the rats treated with sham operation, TBI+ saline, TBI+ rh-EPO solution, TBI+ rh-EPO-Tw-ABNPs. (*P<0.05, **P<0.01, and ***P<0.005, compared with sham group). (**D**) The brain water content of TBI rats at 12, 24, 36 h after administration with saline, or rh-EPO-Tw-ABNPs (2500 IU/kg or 5000 IU/kg), respectively. (*P<0.05, **P<0.01, and ***P<0.005, compared with saline treated group). (**E**) Immunohistochemical image of AQP4 and GFAP in brain tissue section treated with different operations.

tend to develop vasogenic edema.[49,50] In our study, we found that the level of AQP4 expression level decreased under the TBI condition. However, the rh-EPO could recover the AQP4 levels, while the rh-EPO-Tw-ABNPs may further increase the AQP4 level mainly by enhancing the transport of rh-EPO through the Tween 80 modified nanoparticles. We speculated that the rh-EPO formulation could relieve brain edema by reducing vasogenic edema.

GFAP is the main monofilament protein in astrocytes, a specific cytoskeletal protein unique to the CNS, and a marker protein of astrocytes.[51] GFAP can maintain the morphology and function of astrocytes, regulate cell forming, maintain the blood–brain barrier, and produce and release neurotrophic factors.[52,53] It was inferred that the severity of brain injury was positively correlated with GFAP level, that is, the higher the GFAP level, the more serious the brain damage. Pertinently, GFAP has been used to assess brain damage following TBI.[54] The increased expression of GFAP was observed in the TBI group in comparison with the sham-operated batch in our study. This result is consistent with previous research which suggested that TBI may lead to reactive astrogliosis that was characterized by the rapid synthesis of GFAP.[55] Meanwhile, the GFAP levels of rh-EPO solution and rh-EPO-Tw-ABMPs groups declined,

suggesting that EPO could reduce the expression of GFAP. Furthermore, the rh-EPO-Tw-ABMPs group could reduce the GAFP almost to the normal level, thus exhibiting the best therapeutic effect.

H&E

As presented in Figure 6A, the brain tissue of the sham-operated group had no damage focus with complete cortical nerve structure, large number of cells, rich cytoplasm and obvious nucleolus. However, as shown in Figure 6B, the rats in the TBI saline group had cortical structure incomplete, apparent edema, sparse nerve cells, smaller cell volume, widened cell gap, pyknosis nucleus, and non-obvious nucleolus, while cell necrosis was seen in the injury site. Compared with the trauma model group, the injury of neurons in rh-EPO solution group recovered while the tissue edema was reduced (Figure 6C). In the rh-EPO-Tw-ABNPs group, the injury of neurons decreased more significantly, amid the morphology and necrosis of cells being good and reduced respectively, while a large number of new proliferation cells appeared around the trauma (Figure 6D). These results suggest that the inclusion of rh-EPO into albumin nanoparticles modified by Tween 80 may increase the protective effect of rh-EPO on TBI model rats' injury.
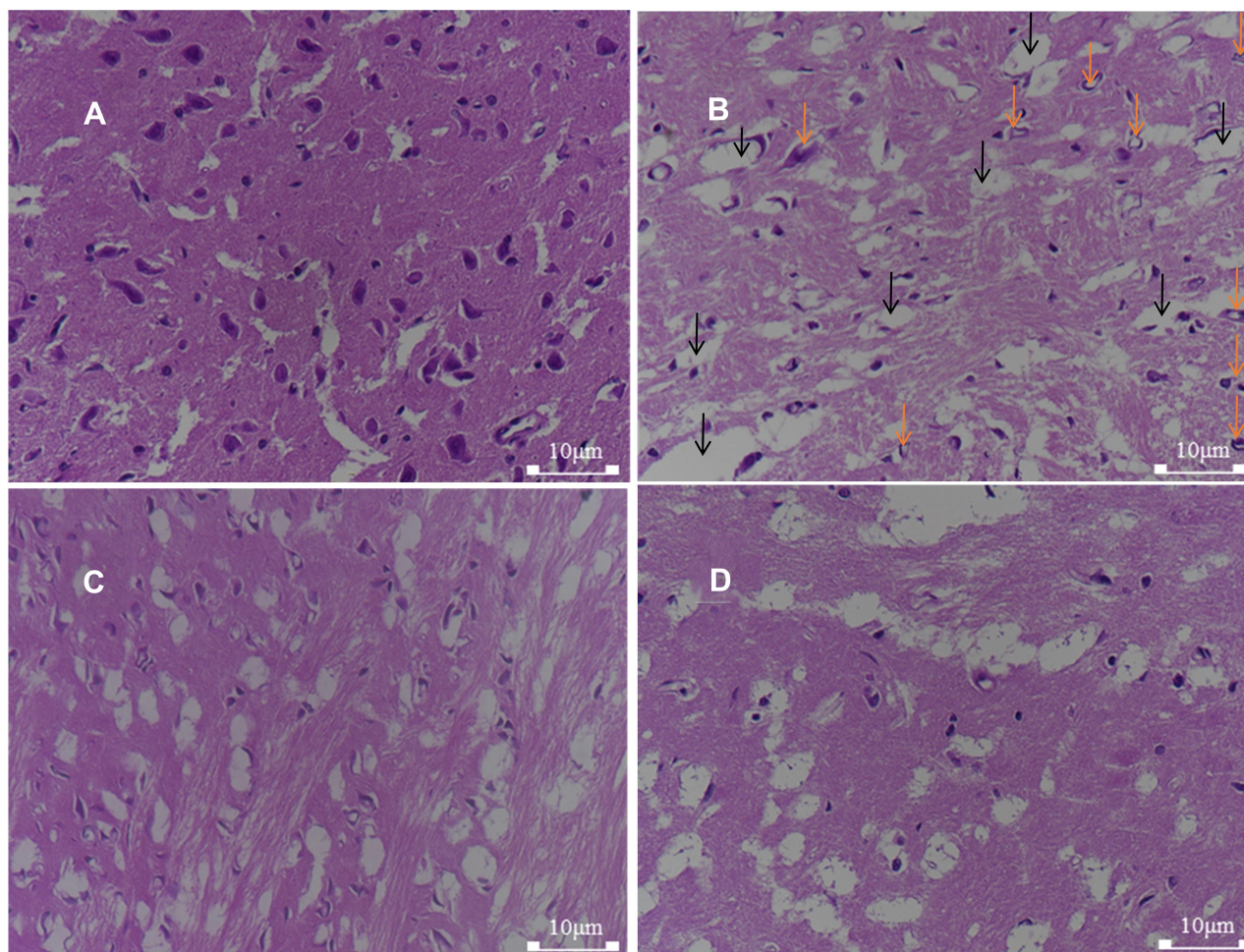
Figure 6 H&E of (**A**) sham operation group; (**B**) TBI+ saline (black arrows show edema and the yellow arrows indicate the pyknosis nucleus in the injury brain); (**C**) rh-EPO solution; (**D**) TBI+ rh-EPO-Tw-ABNPs.

Conclusion

In the present study, a novel rh-EPO-Tw-ABNPs was developed through the application of electrostatic spray technology. The rh-EPO-Tw-ABNPs prepared via optimized formulation exhibited good morphology and ideal particle size, indicating that the electrostatic spray is a potential technology for preparing the protein drug with advantages and feasibility. Furthermore, electrostatic spray technology had few effects on the bioactivity of the protein drug. More importantly, the rh-EPO-Tw-ABNPs could enhance the transport of the rh-EPO into the brain, and relieve TBI symptoms effectively. Therefore, rh-EPO-Tw-ABNPs could serve as a promising formulation for TBI treatment.

Funding

Disclosure

The authors declare no conflicts of interest.

References

1. Kwon EJ, Skalak M, Lo Bu R, et al. Neuron-targeted nanoparticle for siRNA delivery to traumatic brain injuries. *ACS Nano*. 2016;10 (8):7926–7933. doi:10.1021/acsnano.6b03858
2. Han J, Yang S, Zhang C, et al. Impact of intracranial pressure monitoring on prognosis of patients with severe traumatic brain injury: a PRISMA systematic review and meta-analysis. *Medicine (Baltimore)*. 2016;95:e2827. doi:10.1097/MD.0000000000002827
3. Jang SH, Park SM, Kwon HG. Relation between injury of the periaqueductal gray and central pain in patients with mild traumatic brain injury: observational study. *Medicine (Baltimore)*. 2016;95:e4017. doi:10.1097/MD.0000000000004017

4. Abou-Abbass H, Bahmad H, Ghandour H, et al. Epidemiology and clinical characteristics of traumatic brain injury in Lebanon: a systematic review. *Medicine (Baltimore)*. 2016;95:e5342. doi:10.1097/MD.0000000000005342

5. Xiong Y, Mahmood A, Chopp M, et al. Animal models of traumatic brain injury. *Nat Rev Neurosci*. 2013:128–142.

6. Feeney DM, Boyeson MG, Linn RT, et al. Responses to cortical injury: I. Methodology and local effects of contusions in the rat. *Brain Res*. 1981;211(1):67–77. doi:10.1016/0006-8993(81)90067-6

7. Albert-Weissenberger C, Anna-Leena S. Experimental traumatic brain injury. *Exp Transl Stroke Med*. 2010;2:16. doi:10.1186/2040-7378-2-16

8. Si D, Wang H, Wang Q, et al. Progesterone treatment improves cognitive outcome following experimental traumatic brain injury in rats. *Neurosci Lett*. 2013;553:18–23. doi:10.1016/j.neulet.2013.07.052

9. Juul S. Neuroprotective role of erythropoietin in neonates. *J Matern Fetal Med*. 2012;25(S4):97–99.

10. Kumral A, Tüzün F, Meryem Gülfer O, et al. Erythropoietin in neonatal brain protection: the past, the present and the future. *Brain Dev*. 2011;33(8):632–643. doi:10.1016/j.braindev.2010.10.014

11. Wang L, Wang X, Su H, et al. Recombinant human erythropoietin improves the neurofunctional recovery of rats following traumatic brain injury via an increase in circulating endothelial progenitor cells. *Transl Stroke Res*. 2015;6(1):50–59. doi:10.1007/s12975-014-0362-x

12. Blixt J, Gunnarson E, Wanecek M. Erythropoietin attenuates the brain edema response after experimental traumatic brain injury. *J Neurotrauma*. 2018;35(4):671–680. doi:10.1089/neu.2017.5015

13. Verdonck O, Lahrech H, Francony G, et al. Erythropoietin protects from post-traumatic edema in the rat brain. *J Cereb Blood Flow Metab*. 2007;27(7):1369–1376. doi:10.1038/sj.jcbfm.9600443

14. Grasso G, Sfacteria A, Meli F, et al. The role of erythropoietin in neuroprotection: therapeutic perspectives. *Drug News Perspect*. 2007;20(5):315. doi:10.1358/dnp.2007.20.5.1120219

15. Carson KR, Evens AM, Bennett CL, et al. Clinical characteristics of erythropoietin-associated pure red cell aplasia. *Best Pract Res Clin Haematol*. 2005;18(3):467–472. doi:10.1016/j.beha.2005.01.015

16. Yacoby I, Bar H, Benhar I. Targeted drug-carrying bacteriophages as antibacterial nanomedicines. *Antimicrob Agents Chemother*. 2007;51(6):2156–2163. doi:10.1128/AAC.00163-07

17. Dou H, Destache CJ, Morehead JR, et al. Development of a macrophage-based nanoparticle platform for antiretroviral drug delivery. *Blood*. 2006;108(8):2827–2835. doi:10.1182/blood-2006-03-012534

18. Chen H, Spagnoli F, Burris M, et al. Nanoerythropoietin is 10-times more effective than regular erythropoietin in neuroprotection in a neonatal rat model of hypoxia and ischemia. *Stroke*. 2012;43(3):884. doi:10.1161/STROKEAHA.111.637090

19. Wilson B, Samanta MK, Santhi K, et al. Targeted delivery of tacrine into the brain with polysorbate 80-coated poly(n-butylcyanoacrylate) nanoparticles. *Eur J Pharm Biopharm*. 2008;70(1):75–84. doi:10.1016/j.ejpb.2008.03.009

20. Gulyaev AE, Gelperina SE, Skidan IN, et al. Significant transport of doxorubicin into the brain with polysorbate 80-coated nanoparticles. *Pharm Res*. 1999;16(10):1564–1569. doi:10.1023/A:1018983904537

21. Alyautdin RN, Gothier D, Petrov V, et al. Analgesic activity of the hexapeptide dalargin adsorbed on the surface of polysorbate 80-coated poly(butyl cyanoacrylate) nanoparticles. *Eur J Pharm Biopharm*. 1995;41(1).

22. Alyautdin RN, Petrov VE, Langer K, et al. Delivery of loperamide across the blood-brain barrier with polysorbate 80-coated polybutylcyanoacrylate nanoparticles. *Pharm Res*. 1997;14(3):325–328. doi:10.1023/A:1012098005098

23. Alyautdin RN, Tezikov EB, Ramge P, et al. Significant entry of tubocurarine into the brain of rats by adsorption to polysorbate 80–coated polybutylcyanoacrylate nanoparticles: an in situ brain perfusion study. *J Microencapsul*. 1998;15(1):67–74. doi:10.3109/02652049809006836

24. Boda SK, Li X, Xie J. Electrospraying an enabling technology for pharmaceutical and biomedical applications: A review. *J Aerosol Sci*. 2018;125:164–181. doi:10.1016/j.jaerosci.2018.04.002

25. Bock N, Dargaville TR, Woodruff MA. Electrospraying of polymers with therapeutic molecules: state of the art. *Prog Polym Sci*. 2012;37(11):1510–1551. doi:10.1016/j.progpolymsci.2012.03.002

26. Parhizkar M, Reardon PJT, Knowles JC, et al. Performance of novel high throughput multi electrospray systems for forming of polymeric micro/nanoparticles. *Mater Des*. 2017;126(1):73–84. doi:10.1016/j.matdes.2017.04.029

27. Nath SD, Son S, Sadiasa A, et al. Preparation and characterization of PLGA microspheres by the electrospraying method for delivering simvastatin for bone regeneration. *Int J Pharm*. 2013;443(1–2):87–94. doi:10.1016/j.ijpharm.2012.12.037

28. Mehta P, Haj-Ahmad R, Rasekh M, et al. Pharmaceutical and biomaterial engineering via electrohydrodynamic atomization technologies. *Drug Discov Today*. 2016;22(1).

29. Jaworek A. Micro- and nanoparticle production by electrospraying. *Powder Technol*. 2007;176(1):18–35. doi:10.1016/j.powtec.2007.01.035

30. Varshosaz J, Minaiyan M, Dayyani L. Poly(methyl vinyl ether-co-maleic acid) for enhancement of solubility, oral bioavailability and anti-osteoporotic effects of raloxifene hydrochloride. *Eur J Pharm Sci*. 2018;112:195–206. doi:10.1016/j.ejps.2017.11.026

31. Arya N, Chakraborty S, Dube N, et al. Electrospraying: A facile technique for synthesis of chitosan-based micro/nanospheres for drug delivery applications. *J Biomed Mater Res B Appl Biomater*. 2009;88:17–31.

32. Moghadam H, Samimi M, Samimi A, et al. Study of parameters affecting size distribution of beads produced from electro-spray of high viscous liquids. *Iran J Chem Eng*. 2009;6:88–98.

33. Liu H, Du K, Li D, et al. A high bioavailability and sustained-release nano-delivery system for nintedanib based on electrospray technology. *Int J Nanomedicine*. 2018;13:8379.

34. Zhang W, He X. Encapsulation of living cells in small (approximately 100 micron) alginate microcapsules by electrostatic spraying: a parametric study. *J Biomech Eng*. 2009;131(7):074515. doi:10.1115/1.3153326

35. Matabola KP, Moutloali RM. The influence of electrospinning parameters on the morphology and diameter of poly(vinyledene fluoride) nanofibers- effect of sodium chloride. *J Mat Sci*. 2013;48(16):5475–5482.

36. Subbiah T, Bhat GS, Tock RW, et al. Electrospinning of nanofibers. *J Appl Polym Sci*. 2005;96(2):557–569. doi:10.1002/app.21481

37. Antonov YA, Wolf BA, Moldenaers P. Inducing mixing of water-in water BSA/dextran emulsion by a strong polyelectrolyte. *Food Hydrocoll*. 2015;43:243–251. doi:10.1016/j.foodhyd.2014.05.029

38. Li XB, Zheng H, Zhang ZR, et al. Glia activation induced by peripheral administration of aluminum oxide nanoparticles in rat brains. *Nanomedicine*. 2009;5(4):473–479. doi:10.1016/j.nano.2009.01.013

39. Pohland M, Glumm R, Wiekhorst F, et al. Biocompatibility of very small superparamagnetic iron oxide nanoparticles in murine organotypic hippocampal slice cultures and the role of microglia. *Int J Nanomedicine*. 2017;12:1577–1591. doi:10.2147/IJN.S127206

40. Sun W, Xie C, Wang H, et al. Specific role of polysorbate 80 coating on the targeting of nanoparticles to the brain. *Biomaterials*. 2004;25(15):3065–3071. doi:10.1016/j.biomaterials.2003.09.087

41. Zhou ZW, Li F, Zheng ZT, et al. Erythropoietin regulates immune/inflammatory reaction and improves neurological function outcomes in traumatic brain injury. *Brain Behav*. 2017;7(11):e00827. doi:10.1002/brb3.827

42. Yatsiv I, Grigoriadis N, Simeonidou C. Erythropoietin is neuroprotective, improves functional recovery, and reduces neuronal apoptosis and inflammation in a rodent model of experimental closed head injury. *FASEB J*. 2005;19(12):1701–1703. doi:10.1096/fj.05-3907fje

43. Brines ML, Ghezzi P, Keenan S, et al. Erythropoietin crosses the blood-brain barrier to protect against experimental brain injury. *Proc Natl Acad Sci U S A*. 2000;97(19):10526–10531. doi:10.1073/pnas.97.19.10526

44. Barzó P, Marmarou A, Fatouros P, et al. Contribution of vasogenic and cellular edema to traumatic brain swelling measured by diffusion-weighted imaging. *J Neurosurg*. 1997;87(6):900. doi:10.3171/jns.1997.87.6.0900

45. Huang J, Sun SQ, Lu WT, et al. The internalization and lysosomal degradation of brain AQP4 after ischemic injury. *Brain Res*. 2013;1539:61–72. doi:10.1016/j.brainres.2013.09.022

46. Lehmann GL, Gradilone SA, Marinelli RA. Aquaporin water channels in central nervous system. *Curr Neurovasc Res*. 2004;1:293–303. doi:10.2174/1567202043362081

47. Sun MC, Honey CR, Berk C, et al. Regulation of aquaporin-4 in a traumatic brain injury model in rats. *J Neurosurg*. 2003;98(3):565–569. doi:10.3171/jns.2003.98.3.0565

48. Ke C, Poon WS, Ng HK, et al. Heterogeneous responses of aquaporin-4 in oedema formation in a replicated severe traumatic brain injury model in rats. *Neurosci Lett*. 2001;301(1):21–24. doi:10.1016/S0304-3940(01)01589-0

49. Manley GT, Fujimura M, Verkman T, et al. Aquaporin-4 deletion in mice reduces brain edema after acute water intoxication and ischemic stroke. *Nat Med*. 2000;6(2):159–163. doi:10.1038/72256

50. Papadopoulos MC, Manley GT, Krishna S, Verkman AS. Aquaporin-4 facilitates reabsorption of excess fluid in vasogenic brain edema. *FASEB J*. 2004;18(11):1291–1293. doi:10.1096/fj.04-1723fje

51. Pelinka LE, Kroepfl A, Schmidhammer R, et al. Glial fibrillary acidic protein in serum after traumatic brain injury and multiple trauma. *J Trauma Acute Care Surg*. 2004;57(5):1006–1012. doi:10.1097/01.TA.0000108998.48026.C3

52. Zoltewicz JS, Scharf D, Yang B, et al. Characterization of antibodies that detect human GFAP after traumatic brain injury. *Biomark Insights*. 2012;7:71–79. doi:10.4137/BMI.S9873

53. Gwak YS, Kang J, Unabia GC, et al. Spatial and temporal activation of spinal glial cells: role of gliopathy in central neuropathic pain following spinal cord injury in rats. *Exp Neurol*. 2012;234(2):362–372. doi:10.1016/j.expneurol.2011.10.010

54. Metting Z, Wilczak N, Rodiger LA, et al. GFAP and S100B in the acute phase of mild traumatic brain injury. *Neurology*. 2012;78(18):1428–1433. doi:10.1212/WNL.0b013e318253d5c7

55. Zhang B, Wang B, Cao S, et al. Epigallocatechin-3-Gallate (EGCG) attenuates traumatic brain injury by inhibition of edema formation and oxidative stress. *Korean J Physiol Pharmacol*. 2015;19(6):491–497.